Surface reconstructions and atomic ordering in In$_x$Ga$_{1-x}$As(001) films: A density-functional theory study

Aparna Chakrabarti,[1] Peter Kratzer,[2,3] and Matthias Scheffler[2]

[1]*Raja Ramanna Centre for Advanced Technology, Indore 452013, India*

[2]*Fritz-Haber-Institut der Max-Planck-Gesellschaft, Faradayweg 4-6, D-14195 Berlin, Germany*

[3]*Fachbereich Physik, Universität Duisburg-Essen, Lotharstrasse 1, D-47048 Duisburg, Germany*

Density-functional theory calculations were carried out for various surface reconstructions of atomically ordered thin films of In$_x$Ga$_{1-x}$As on the InP(001) substrate for compositions close to $x=1/2$. In addition to the known $(n \times 3)$ and (2×4) reconstructions, a gallium-rich $\zeta(4 \times 2)$ reconstruction, so far only observed for binary arsenides, is predicted. Moreover, the possibility of a $c(4 \times 4)$ reconstruction, either purely terminated by As-As dimers or mixed with heterodimers, as well as the possible occurrence of heterodimers in other reconstructions have been investigated. From our calculated film formation energies, these reconstructions are expected to play a minor role for In$_x$Ga$_{1-x}$As films under thermodynamic equilibrium conditions. For the surface-induced atomic ordering in the In$_x$Ga$_{1-x}$As films, our calculations are in line with known trends for In$_x$Ga$_{1-x}$P alloys. In general, the energetic preference for near-surface ordering in the In$_x$Ga$_{1-x}$As system is found to be somewhat weaker than in the In$_x$Ga$_{1-x}$P system.

I. INTRODUCTION

Ternary compound semiconductors from elements of groups III and V in the periodic table are interesting materials, both in view of applications and fundamental research. Ternary compound semiconductors offer enhanced flexibility compared to binary III-V compounds to tune materials properties, in particular the optical band gap. Thin films and quantum well systems of ternary compounds can be fabricated by epitaxial growth techniques if a suitable lattice-matched substrate is available. This is possible in particular for In$_x$Ga$_{1-x}$P films on GaAs and for In$_x$Ga$_{1-x}$As films on InP, materials that are closely lattice-matched if the ternary film contains about equal amounts of both cations. A large body of literature exists (see citations in Refs. 1 and 2) reporting experimental observations of the cations in zinc-blende-type compounds In$_x$Ga$_{1-x}$P and In$_x$Ga$_{1-x}$As occupying distinct sublattices of the face-centered cubic (fcc) cation lattice. For alloy films grown on (001)-oriented substrates, ordering of the copper-platinum (CuPt)-type is observed most frequently (a superlattice of alternating InAs and GaAs monolayers along the $\langle 111 \rangle$ cubic body diagonals, named in analogy to ordered structures in fcc-metal alloys). Of the four bulk-equivalent body diagonals, ordering has been seen to take place along either the two directions $[\bar{1}11]$ and $[1\bar{1}1]$ (called CuPt$_B$ variant), or the other two directions $[111]$ and $[\bar{1}\bar{1}1]$ (called CuPt$_A$ variant). For anion-terminated surfaces, a triple-period-ordering leading to a $(n \times 3)$ (where $n=1,2,4$) surface reconstruction has also been observed.[3–6,8,9] Calculations have shown the formation of ordered ternary alloys from the corresponding binary compound semiconductors to be endothermic.[10] The occurrence of the ordering is apparently related to the epitaxial growth process and the prevailing surface reconstructions. Identifying suitable growth conditions is of considerable interest, as the atomic-scale ordering has important consequences for the optical and electronic properties. Experimentally, CuPt-type atomic

ordering in III-V alloys has been observed to reduce the band gap by several tens to hundreds of meV.[11–14] Theoretical studies on band gap lowering for most III-V and II-VI ordered alloys (with respect to their random structural variant) have been reported in the literature.[15,16]

In the present article, we report first-principles calculations aimed at clarifying the surface reconstructions and the atomic orderings in ternary In$_x$Ga$_{1-x}$As epilayers on InP(001). Compared to In$_x$Ga$_{1-x}$P alloys, In$_x$Ga$_{1-x}$As alloys have received less attention so far from the theoretical side. Moreover, interesting new types of reconstructions have been reported recently for the (001) surface of III-V binary compounds.[17–20] These studies include the $\zeta(4 \times 2)$ reconstruction for the As-poor GaAs(001) surface,[17] and the observation of heterodimers on the As-rich $c(4 \times 4)$ reconstruction of GaAs(001),[18] as well as cation-rich reconstructions of binary and ternary phosphides.[19,20] We want to clarify by means of total-energy calculations whether the trend established for the well-studied ternary phosphides (see, e.g., Ref. 21) carry over to the In$_x$Ga$_{1-x}$As system, and how the surface reconstructions identified recently for binary compounds can affect ordering in this material system.

From the theoretical point of view, the occurrence of ordering in epitaxially grown films has been understood as the result of surface thermodynamics as opposed to bulk thermodynamics. Depending on the surface reconstruction, there is a small but notable energetic preference for the cation lattice sites in the surface and subsurface layers to be occupied by either Ga or In atoms, e.g., due to local variations of bond lengths. While energetically very unfavorable defects, e.g., antisites, are strongly suppressed during high-temperature growth and equilibrium with respect to the stoichiometry is established between bulk and surface, the energy differences in the bulk associated with ordering on the cation lattice are too small to act as an efficient driving force for equilibration. Hence, In and Ga atoms are likely to remain on the sites dictated by the surface reconstruction as growth proceeds.[1]

Moreover, it has been argued that atom diffusion could occur more easily near the surface than in the bulk, thus leading to efficient equilibration only within the topmost layers.[22,23] When this scenario is operative, the formation energy of a very thin film (representative of the near-surface layers equilibrated during the growth process) is indicative of the stability of an atomic ordering pattern in conjunction with a specific surface reconstruction. In a certain sense, one could say that surface thermodynamics is the cause of this atomic ordering, while the growth kinetics is the carrier or the propagator of it.[1] For films of ternary III-V compounds, these ideas have been worked out for the example of $In_xGa_{1-x}P$ films in a number of works by Zunger and his group.[21] By means of first-principles calculations of the ordering energy (i.e., the difference in energy between the ordered alloy and the disordered or random alloy) they could establish a connection between surface thermodynamics and the experimental observation of a one-to-one correspondence between a particular surface reconstruction and a particular ordering pattern.[1,2] For example, while the most well-studied $CuPt_B$-type ordering is observed for the $\beta2(2\times4)$ surface reconstruction, the $c(4\times4)$ reconstruction is always associated with $CuPt_A$-type ordering: The presence and the orientation of the top anion dimers in the surface reconstruction of the alloy films affect the preferred subsurface sites of the cations, and in turn the direction of crystal planes for which ordering occurs. First-principles calculations[21] indicated that the anion-rich $c(4\times4)$ or $(n\times3)$ reconstructions, and hence $CuPt_A$-type and triple-period ordering, respectively, should be favorable for higher concentration of anions on the surface. Obtaining these reconstructions requires growth in a narrow temperature window, as achieved experimentally, e.g., by Gomyo et al.[3,24]

In this paper, we aim at a comprehensive investigation of the reconstructions of the surface of $In_xGa_{1-x}As(001)$ alloy films with nearly equal concentrations of the cations In and Ga. We probe the stabilities of the following types of major reconstructions $\alpha2(2\times4)$, $\beta2(2\times4)$, $\zeta(4\times2)$, $c(4\times4)$, (2×3), and (4×3). For each lateral periodicity, several realizations of the reconstruction are considered, including those with heterodimers. We have also taken ordering in the cation sublattice into account for all the reconstructions. Whenever information is available from previously studied $In_xGa_{1-x}P$ alloy films,[1,2] we use it for the type of atomic ordering accompanying the reconstruction. For the observed reconstructions of $In_xGa_{1-x}As$, where no information is available, we test several possible ordering patterns to find the energetically most favorable one. In Sec. II, the method for calculating film formation energies (denoted by the symbol γ) is described, and an expression for the thermodynamic stability is derived, represented in our calculational method by the values of the chemical potentials of the atomic species. Subsequently, we present the atomic geometries of the reconstructions and discuss their stability at zero temperature (Sec. III A). In Sec. III B, we compare the energetics of different ordering patterns for selected surface reconstructions. This is aimed at probing the extent of interplay between the surface reconstruction and ordering in $In_xGa_{1-x}As$. Finally, we present our conclusions.

II. CALCULATIONAL METHOD

In this work, we employ total-energy calculations within density-functional theory[25] (DFT) with the local-density approximation for the exchange-correlation energy functional.[26] The pseudopotential-plane-wave approach (FHIMD code[27]) is used with norm-conserving fully separable pseudopotentials.[28] The wavefunctions are expanded into plane waves with an energy cutoff of 10 Ry. The Brillouin zone (BZ) integration of the electron density is performed using a Monkhorst-Pack mesh equivalent to at least 64 k points in the 1×1 surface BZ.[29] We report calculations for a slab of 12 atomic layers used for the simulation of the alloy films (apart from very arsenic-rich surface reconstructions that have an additional layer of arsenic, and thus 13 layers in total). For the InP substrate, four atomic layers are considered, with a phosphorous layer forming the interface to the $In_xGa_{1-x}As$ alloy. A sufficiently large vacuum region (corresponding to 12 atomic layers) separates the periodic images of the slabs in adjacent supercells. One side of the slab is used to model the surface reconstruction to be studied. The other side, terminating in a layer of In atoms, was passivated by pseudohydrogen atoms with a nuclear charge $Z=1.25$, to mimic continuation of the substrate by a phosphorous layer. Along the lateral direction (i.e., along the x and y axes), the calculated substrate lattice constant is used. The slab is electrically neutral but as a consequence of its nonsymmetric construction, it has a dipole moment which is compensated by using a dipole correction.[30] With this treatment the artificial electrostatic interaction between the surfaces through the vacuum region is canceled. To obtain the equilibrium structure, the whole alloy film along with the two upper atomic layers of the four-layer-thick substrate is relaxed until the forces are negligible (below 0.01 eV/Å). The bottom layer of the substrate and the pseudohydrogen layer are kept fixed. For subtraction of the energy contribution of the fixed substrate layers and the pseudohydrogen, a separate calculation is performed for a symmetric slab where both sides are pseudohydrogen terminated. The remaining energy is denoted by E_{tot}. The formation energies of the alloy films for different surface reconstructions, denoted by γ, are obtained by subtracting from E_{tot} the total energy of an appropriate amount of bulk material (see below).

For the discussion below concerning the stability of the films it is assumed that thermodynamic equilibrium has been reached. Experimentally, this can be achieved by annealing the films under arsenic flux. Under equilibrium conditions, the formation energy of a thin alloy film as calculated below is indicative of the stability of a certain type of ordering and reconstruction. In some cases, evidence has been given that GaAs growth experiments were conducted close to equilibrium.[31] Coming close to equilibrium conditions implies a relatively high temperature and arsenic pressure (comparable to the vapor pressure of GaAs at this temperature), and a low deposition flux of Ga and In atoms, such that the equilibrium concentrations of Ga and In adatoms on the substrate surface are only weakly perturbed by this external flux. However, it is to be recalled that growth may be controlled not only by thermodynamics but also by various kinetic factors, which are beyond the scope of the present study.

Both for annealing under an arsenic flux and during growth, the arsenic flux (typically 10–50 particles per lattice site per second) is much higher than the flux of the cations, In or Ga, and there is both adsorption and desorption of arsenic molecules in nearly equal amounts. Therefore, we choose μ_{As}, the arsenic chemical potential, as one thermodynamic variable. The average chemical potential of the cations is then fixed by requiring the overall composition of anions and cations to be in equilibrium with the bulk alloy. For $In_{0.5}Ga_{0.5}As$, the ordered alloy structure with the lowest energy is the chalkopyrite structure. According to our calculations, its heat of formation from the elements[32] at zero temperature is −0.48 eV per formula unit. This is slightly less than the average of the calculated heat of formation of GaAs and InAs, $\Delta H(GaAs)=-0.72$ eV and $\Delta H(InAs)=-0.29$ eV, respectively. Hence, alloy formation is endothermic. For thin alloy films, the observed alloy ordering is of the CuPt type, which we calculate to be even slightly more unfavorable than the chalkopyrite-type ordering, by 0.06 eV per formula unit. The observed formation of the CuPt alloy in thin films can thus only be explained by the interplay between surface reconstructions and subsurface ordering of the cations, as discussed in the Introduction. In the following, we choose the heat of formation of the ordered compound with the highest relative stability, $In_{0.5}Ga_{0.5}As$ with chalkopyrite ordering, to fix the average chemical potentials of the cations, because an alloy with local structure similar to chalkopyrite would result after annealing of thick films

$$0.5(\mu_{Ga} + \mu_{In}) + \mu_{As} = E^{chalko}_{In_{0.5}Ga_{0.5}As(bulk)}. \quad (1)$$

Since the bulk alloys in question (but not necessarily the thin films) contain Ga and In in equal amounts, it is convenient to take $\mu_{Ga}-\mu_{In}$ as the second variable, in addition to μ_{As}. The dependence of the film formation energy upon the difference of the In and Ga chemical potentials indicates how sensitive the film formation is with respect to composition fluctuations of the cations. Evaluating all contributions at $T=0$ K, we obtain the following expression for γ, the film formation energy:

$$\gamma A = E_{tot} - (N_{Ga} + N_{In})E^{chalko}_{In_{0.5}Ga_{0.5}As(bulk)}$$

$$- \frac{1}{2}(N_{Ga} - N_{In})[\mu_{In} - \mu_{In(bulk)} - (\mu_{Ga} - \mu_{Ga(bulk)})]$$

$$- (N_{As} - N_{Ga} - N_{In})(\mu_{As} - \mu_{As(bulk)}). \quad (2)$$

Here, E_{tot} is the total energy of the slab calculated within DFT, approximated by its value at $T=0$ K. $\mu_{In(bulk)}$, $\mu_{Ga(bulk)}$, and $\mu_{As(bulk)}$ are the chemical potentials of these species in their corresponding bulk reservoirs, and at $T=0$ K we substitute them by $E_{In(bulk)}$, $E_{Ga(bulk)}$, and $E_{As(bulk)}$, the cohesive energies of the respective bulk phases. N_{Ga}, N_{In}, and N_{As} are the numbers of Ga, In, and As atoms in the unit cell, and A is its area. Introducing the abbreviation $\Delta\mu=\mu_{In}-\mu_{In(bulk)}-(\mu_{Ga}-\mu_{Ga(bulk)})$, the formation energy of the alloy film is denoted as a function of two variables $\gamma(\mu_{As},\Delta\mu)$. From plots of $\gamma(\mu_{As},\Delta\mu)$ versus the chemical potentials, it is possible to assess the stability of reconstructions, and thus to

predict the related ordering pattern formed in the alloy films, when the arguments given in the Introduction are applicable. We note that $\gamma(\mu_{As},\Delta\mu)$ includes contributions of the surface, of the interface to the substrate, and of elastic strain due to mismatch of the lattice constant of the $In_xGa_{1-x}As$ alloy with the InP substrate lattice constant. In the present study, we are interested in $In_xGa_{1-x}As$ alloys with nearly equal amounts of Ga and In. For these compositions, the alloy lattice constant is close to the lattice constant of the substrate used in our calculations, InP(001). Hence we expect elastic strain contributions to be small; yet they are included in the following formation energies. For this reason, the formation energies are in general dependent on film thickness, and the numbers given below are valid only for films of the specified thickness, 12 layers. However, the reported occurrence of different surface reconstructions as well as the correlations between surface reconstruction and alloy ordering, are valid also for thicker films.

III. RESULTS AND DISCUSSION

First, we describe the geometry of the various surface reconstructions included in this study. For all those reconstructions where ordering of the subsurface cation sublattice has been studied for $In_xGa_{1-x}P$ alloys, we used the analogous cation arrangement for $In_xGa_{1-x}As$. Supplementary calculations using different ordering patterns are reported in Sec. III B.

We start with arsenic-rich surfaces with an additional layer of arsenic dimers on the terminating arsenic layer of the alloy. For this termination, the $c(4\times4)$, as well as a variety of $(n\times3)$ reconstructions [either (1×3), (2×3), or (4×3)] were reported for $In_xGa_{1-x}As$ *surface* alloys.[4–7] As shown in Fig. 1, the (2×3) reconstruction has two As-As dimers as an ad-layer, together with one As-As dimer formed in the uppermost full As layer (below the top layer). Figure 1(a) gives the side view of this anion-rich (2×3) reconstruction, where it is observed that the smaller Ga atom occupies the cation site below the As-As dimer, while the larger In atoms occupy the two cation sites below the trench. This gives rise to a triple-period ordering of the alloy, as reported earlier.[5] Figure 1(b) shows two surface unit cells of the same reconstruction in top view. The As-As ad-dimer bonds are shown in black. Furthermore, we investigate three different types of (4×3) reconstructions. The simplest one, containing only As-As dimers, and denoted below by (4×3), has been proposed by Ohkouchi and Gomyo.[8] In addition, we consider reconstructions with In-As and Ga-As heterodimers, namely, the $\alpha(4\times3)$ and $\beta(4\times3)$ reconstructions, as given in the literature for binary antimonides.[33] The "plain" (4×3) is similar to the (2×3) reconstruction, with the only difference that there are groups of three As-As dimers alternating with a gap instead of a complete As-As dimer row. In the $\beta(4\times3)$ surface, this gap is filled by an additional cation-anion ad-dimer (shifted with respect to the As-As ad-dimers, see Ref. 33). The $\alpha(4\times3)$ surface is similar to the $\beta(4\times3)$ surface, except having four cation-anion dimers instead of three As-As dimers plus one anion-cation ad-dimer, see Ref. 33. Our cal-
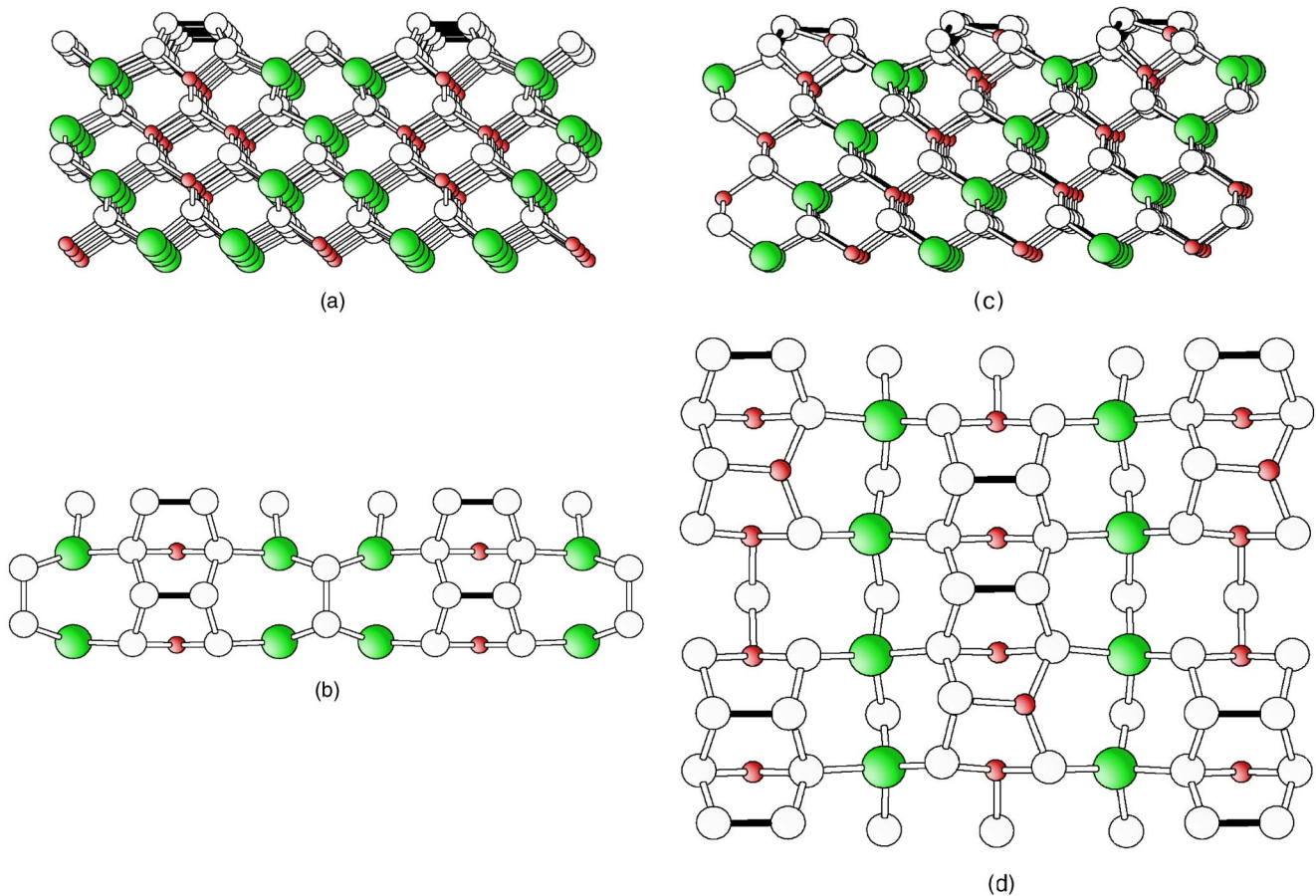
FIG. 1. (Color online) (a) Side view of the anion-rich (2×3) reconstruction, consisting of an anion-anion dimer and a trench region. It is observed that the smaller Ga atom (smallest sphere, red) occupies the cation site below the dimer of As atoms (empty sphere); while the larger In atoms (largest sphere, green) occupy the two cation sites below the trench region. This gives rise to the triple-period ordering of the alloy represented by a 2:1 ratio of the two types of cations in each cation row. (b) Two surface unit cells of the same reconstruction in top view. The As-As ad-dimer bonds on the topmost surface layer are shown in black. (c) Side view of a reconstruction with $c(4\times4)$ periodicity, with two As-As dimers and one Ga-As dimer on the top. As in (2×3) reconstruction, the smaller Ga atoms occupy the cation sites below the As dimers, while the larger In atoms occupy the cation site between dimers. This gives rise to the CuPt$_A$ ordering represented by a 1:1 ratio of the two types of cations in each cation row. (d) The same reconstruction from top. The As-As and Ga-As ad-dimer bonds on the topmost surface layer are shown in black and white, respectively.

culations show that cation-anion ad-dimers with Ga as the cation are energetically more favorable compared to the ones with In as the cation. The probable reason may be that the atomic radii of Ga and As are comparable, while the atomic radius of In is larger with respect to As. Hence in discussing the results below, we concentrate on the former case (Ga-As heterodimers). In the (4×3) reconstructions, similar to the (2×3) reconstruction, tensile surface stress due to surface dimer formation favors the smaller Ga atom sitting below the dimers and the larger In atom sitting between the dimers in the subsurface cation layer. This mechanism acts as driving force for the triple-period ordering, exactly as found in case of the (2×3) reconstruction.

Now we turn to anion-rich surfaces with $c(4\times4)$ unit cell. Figure 1(c) shows the side view of a reconstruction with $c(4\times4)$ periodicity, with two As-As dimers and one Ga-As dimer on the top. In Fig. 1(d), we view the same reconstruction from top. This reconstruction is hereafter referred to as $c(4\times4)$-GaAs-1hd, while the reconstruction referred to be-

low as $c(4\times4)$ has the same surface structure but with three pure As-As dimers instead of two As-As dimers and one heterodimer. Following previous work for the $c(4\times4)$ heterodimer reconstructions on pure GaAs films,[34] we consider it sufficient to investigate only the case where the heterodimer is at the end of the three-dimer group, since having the heterodimer in the middle offers less possibility for structural relaxation and was thus found to be higher in energy. For pure GaAs films, experiments have also observed $c(4\times4)$ reconstructions with three heterodimers.[18] Motivated by this observation, we also include the $c(4\times4)$-GaAs-3hd and $c(4\times4)$-InAs-3hd reconstructions in our study of In$_x$Ga$_{1-x}$As alloy films. For all the arsenic-rich reconstructions described so far, the bond axis of the ad-dimers points in the [110] direction, giving rise to tensile surface stress in this direction. The normal vector of the crystal plane on which ordering occurs must have a component parallel to the stress direction. For this reason, the cations order in (111) planes for thin films with the $c(4\times4)$ reconstruction. This
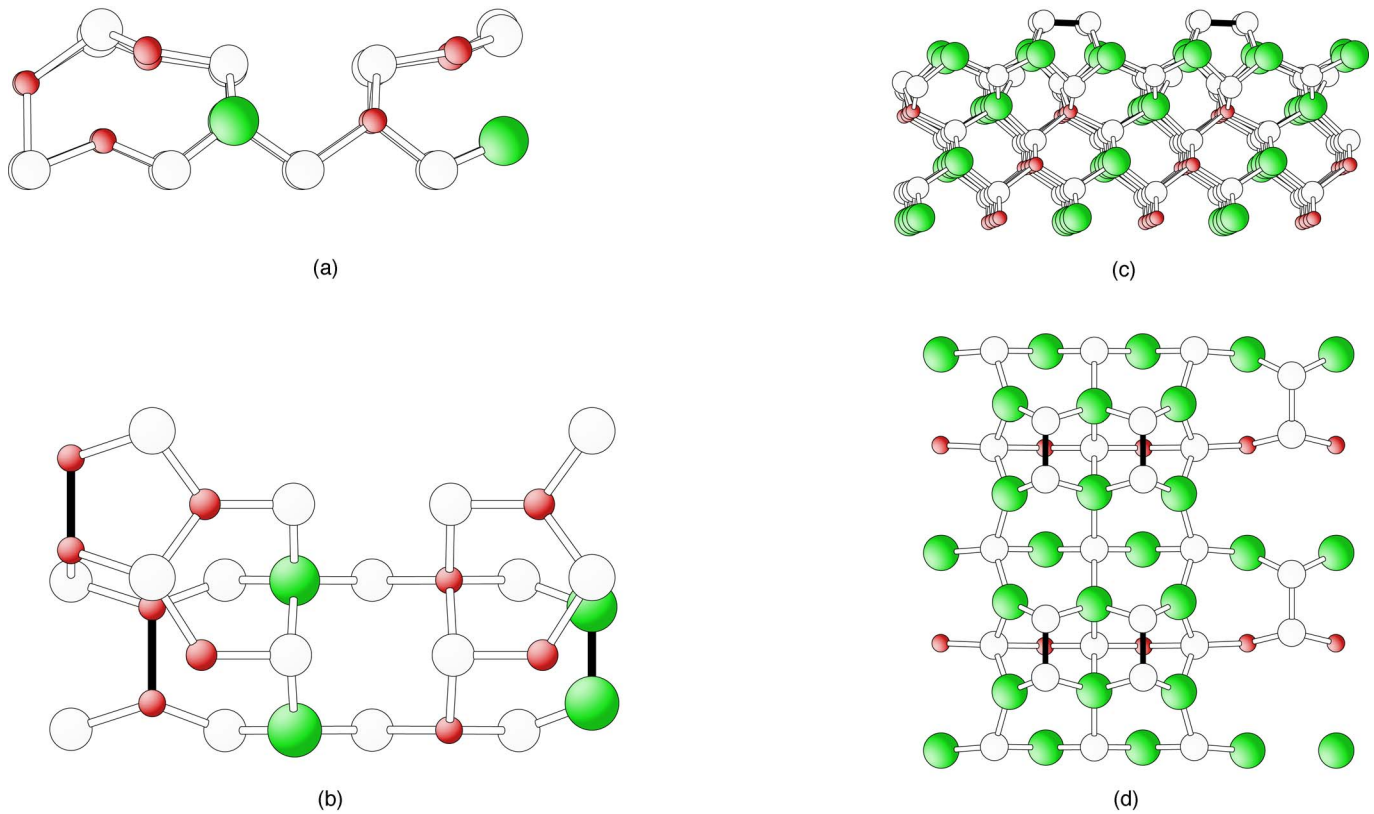
(a)

(b)

(c)

(d)

FIG. 2. (Color online) (a) Side view of the $\zeta(4\times2)$ reconstruction, with CuPt$_B$ ordering (see results and discussion). The top layer contains two zig-zag chains of anions and cations per unit cell. In the subsurface layer, we find three cation-cation dimers, two of them right below the two zig-zag chains, and one between them. (b) Top view of the same reconstruction. Two Ga-Ga (smallest atom, red) dimers and one In-In (largest atom, green) dimer bonds are shown in black. (c) Side view of the $\beta2(2\times4)$ reconstruction, with CuPt$_B$ ordering (d) top view of the same reconstruction. Both the topmost arsenic (empty sphere) layer and the second (cation) layer are incomplete, and the former one contains two As-As dimers with their bond axis oriented along the $(1\bar{1}0)$ direction. The dimer bonds are shown in black. The incomplete surface layer results in trenches running in the $(1\bar{1}0)$ direction where As atoms from the third layer are visible and form a third As-As dimer (seen on the right side in top view).

type is called the CuPt$_A$-type ordering in the literature,[1,2] to distinguish it from CuPt$_B$-type ordering, where the cations occupy $(\bar{1}\bar{1}1)$ crystal planes.

In Fig. 2, we show reconstructions which are moderately As-rich, or cation-rich, namely, the $\beta2(2\times4)$ and $\zeta(4\times2)$ reconstructions, respectively. The $\zeta(4\times2)$ reconstruction[17,35] has been shown to be the stable surface structure for the GaAs(001) surface under As-poor conditions. This finding motivated us to test its stability for the In$_x$Ga$_{1-x}$As(001) surface as well. Figure 2(a) gives the side view of the $\zeta(4\times2)$ reconstruction, while Fig. 2(b) gives the top view. The topmost layer contains two zig-zag chains of anions and cations per unit cell. In the subsurface layer we find three cation-cation dimers, two of them right below the two zig-zag chains, and one between them. This subsurface cation dimerization for the (4×2) reconstruction has been reported recently in the literature.[17,35] In the absence of information in the literature about cation sublattice ordering for the $\zeta(4\times2)$ reconstruction, we have tested various possible ordering patterns and established which is energetically the most stable one. This is the one shown in Fig. 2: One of the three subsurface cation dimers is an In-In dimer, while the others are Ga-Ga dimers. In the deeper cation layers, the $(\bar{1}\bar{1}1)$

crystal planes are alternatingly occupied by Ga and In atoms, i.e., the ordering of the thin film is of CuPt$_B$ type. The incomplete bonding in the top-most layer leaves a trench running in (110) direction, as observed from the side view in Fig. 2(a). Since this trench gives room for structural relaxation, we find it to be more favorable for the larger In atoms to sit below the trench region, and for the smaller Ga atoms to sit between the trench regions. We have also considered the possibility of In segregation in the $\zeta(4\times2)$ reconstruction: the topmost cation layer with normal fourfold coordination consists of only In atoms in this case, referred to as $\zeta(4\times2)$-In-seg, while the subsurface cation dimer layer is as in the standard $\zeta(4\times2)$ reconstruction.

Next, we describe several reconstructions being stoichiometric or moderately As rich, the $\alpha2(2\times4)$ and $\beta2(2\times4)$ reconstructions. Figures 2(c) and 2(d) show the side and top view of the $\beta2(2\times4)$ reconstruction. Both the topmost arsenic layer and the second (cation) layer are incomplete, and the former one contains two As-As dimers with their bond axis oriented along the $(1\bar{1}0)$ direction. The incomplete surface layer results in trenches running in the $(1\bar{1}0)$ direction where As atoms from the third layer are visible and form a third As-As dimer [seen on the right side in Fig. 2(d)]. The

$\alpha2(2\times4)$ reconstruction is similar to the $\beta2(2\times4)$ reconstruction, but has a complete cation layer. Hence the As-As dimer in the trench is not present, instead two cation-cation bonds are formed. While the $\beta2(2\times4)$ is moderately As-rich, the $\alpha2(2\times4)$ reconstruction has equal amounts of anions and cations. Recently, Millunchick et al.[36] reported $\alpha2(2\times4)$ and $\beta2(2\times4)$ reconstructions enriched in In. Hence we have considered In surface segregation, meaning that the top cation layer contains only In atoms, in both the reconstructions, in conformity with the literature.[1,2,37] These reconstructions are labeled $\alpha2(2\times4)$-In-seg and $\beta2(2\times4)$-In-seg in the following discussion. Similarly, the reconstructions labeled $\alpha2(2\times4)$-Ga-seg, $\beta2(2\times4)$-Ga-seg, $\alpha2(2\times4)$, and $\beta2(2\times4)$ have their topmost cation layer consisting fully of Ga in the first two cases, or have no segregation, i.e., a mixed cation layer, in the latter two cases. Drawing inspiration from recent experimental and theoretical studies,[18,34] we have also considered $\alpha2(2\times4)$ and $\beta2(2\times4)$ reconstructions with two or one of the top surface anion dimers replaced by cation-anion heterodimers. For the former variants, we use suffixes "GaAs" or "InAs" to specify the nature of the heterodimer, while the variants with only one heterodimer have an additional "hd" appended. In addition, we studied $\beta2(2\times4)$ reconstructions labeled "md" and "MDd," where "md" stands for one In-In or Ga-Ga dimer replacing an As-As dimer, and "MDd" stands for one mixed metal dimer of In-Ga type replacing an As-As dimer; both along with one remaining As-As dimer. Different from the above structures, a reconstruction with (2×4) periodicity and cation-anion heterodimer has also been suggested by Schmidt et al. for InP(001) surfaces, on the basis of STM and SXPS data.[20] We include this so-called mixed-dimer model into our investigations of the stability of $In_xGa_{1-x}As$ alloy films. For the cation of the cation-anion dimer, we consider either Ga or In, in the following denoted by (2×4)-GaAs and (2×4)-InAs, respectively. We have studied two variants of each structure, one with surface segregation of In [labeled (2×4)-InAs-In-seg] and one without any surface segregation [labeled (2×4)-InAs], for the In-As mixed dimer case. Similarly, two variants for Ga-As mixed-dimer reconstruction have been calculated as well.

In all (2×4) reconstructions considered here, including the (2×4) mixed-dimer reconstruction,[20] the $\alpha2(2\times4)$ and $\beta2(2\times4)$ reconstructions with either anion dimers or heterodimers, these dimers have their bond axis pointing in $(1\bar{1}0)$ direction. Due to the stress exerted on the surface, the crystal planes on which the cation ordering occurs are the $(\bar{1}\bar{1}1)$ planes. This type of ordering is called the $CuPt_B$-type ordering in the literature.[1,2]

A. Stability diagram at zero temperature

In order to predict the surface reconstructions of alloy films under equilibrium conditions, the structure with the minimum formation energy $\gamma(\mu_{As}, \Delta\mu)$ for a given pair of variables is sought. The respective structures are displayed in the stability diagram at zero temperature, Fig. 3, for a 12-layer $In_xGa_{1-x}As$ film as function of the chemical potential of
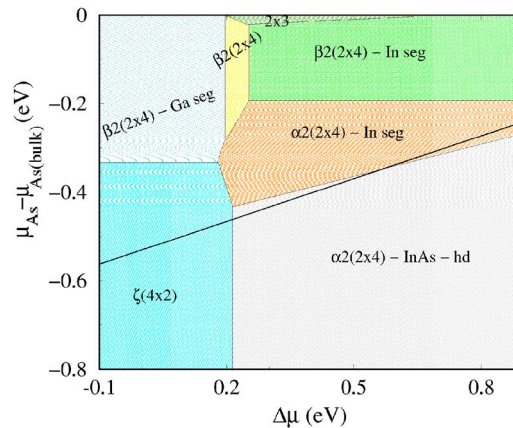

FIG. 3. (Color online) Stability diagram for a 12-layer $In_xGa_{1-x}As$ film as function of the chemical potential of arsenic (with respect to its bulk value), $\mu_{As}-\mu_{As(bulk)}$, and the chemical potential difference of indium and gallium, both with respect to their bulk values, $\Delta\mu = \mu_{In}-\mu_{In(bulk)}-(\mu_{Ga}-\mu_{Ga(bulk)})$. The vertical axis corresponds to the anion chemical potential, whereas the horizontal axis represents the chemical potential difference of the two cations. To avoid precipitation of the binary materials, the variable $\Delta\mu$, describing composition fluctuations, may vary only over a limited range. In one limit, the $In_xGa_{1-x}As$ film is in equilibrium with bulk InAs, and in the other limit, it is in equilibrium with bulk GaAs. The midpoint is chosen such as to correspond to equal concentrations of indium and gallium, which has the value of $\Delta\mu = \Delta H(InAs)-\Delta H(GaAs) \sim 0.43$ eV. The inclined line crossing the diagram indicates the thermodynamic stability limit of the compounds against decomposition into the elements. The stability diagram gives the most stable reconstructions in the various ranges of chemical potentials within the respective limits, as discussed above.

arsenic μ_{As}, and the chemical potential difference of indium and gallium, both with respect to their bulk values $\Delta\mu = \mu_{In}-\mu_{In(bulk)}-(\mu_{Ga}-\mu_{Ga(bulk)})$. The vertical axis corresponds to the anion chemical potential, whereas the horizontal axis represents the chemical potential difference of the two cations. The variable $\Delta\mu$, describing composition fluctuations, may vary only over a limited range. In one limit, the $In_xGa_{1-x}As$ film is in equilibrium with bulk InAs, and in the other limit, it is in equilibrium with bulk GaAs. For the range shown in Fig. 3, the midpoint is chosen such as to correspond to equal concentrations of indium and gallium. Inserting values yields $\Delta\mu = \Delta H(InAs)-\Delta H(GaAs) = 0.43$ eV. Deviations of $\Delta\mu$ to either side for nonstoichiometric alloys must not be larger in magnitude than the heat of formation of the alloy. Hence Ga-rich alloy films will correspond to small negative values of $\Delta\mu \sim -0.1$ eV, while for In-rich alloys this variable may not exceed ~ 0.9 eV. The range of $\Delta\mu$ displayed in Fig. 3 corresponds to the abovementioned bounds.

In the top region of Fig. 3, within a very small range of very high chemical potential of As and In, the experimentally observed (2×3) reconstruction[4,5] is seen to be stable. The double anion layer on this surface makes it very As-rich and hence favorable at a high chemical potential of As. Further on, the calculated film formation energy per unit area, $\gamma(\mu_{As}, \Delta\mu)$ indicates that a chemical environment both rich in Ga and As helps to stabilize the $\beta2(2\times4)$-Ga-seg. recon-
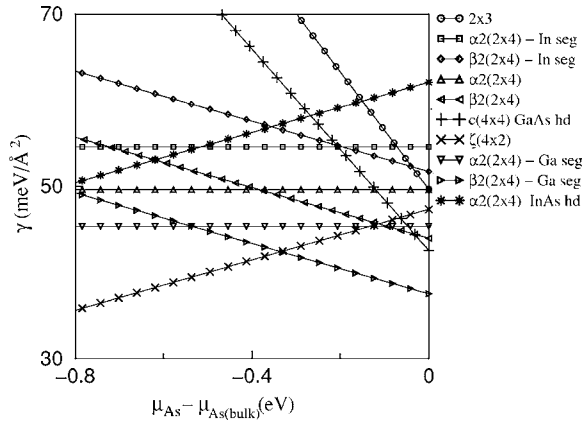
FIG. 4. Formation energies of some important and more stable reconstructions as a function of As chemical potential for Ga-rich alloy composition, $\Delta\mu=-0.1$ eV. This corresponds to one vertical line from the stability diagram, Fig. 3 (the left y axis).
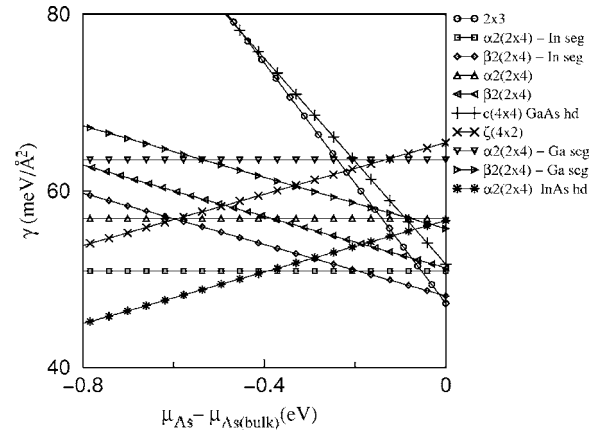

FIG. 5. Formation energies of some important and more stable reconstructions as a function of As chemical potential for equal concentrations of the two cations ($\Delta\mu=0.4$ eV). This corresponds to one vertical line from the stability diagram, Fig. 3.

struction. Under the same conditions, a $c(4\times4)$-GaAs-1hd reconstruction has a comparably low, but slightly higher surface energy, than the $\beta2(2\times4)$ as is observed from Fig. 4, which shows formation energies for Ga-rich alloy composition $\Delta\mu=-0.1$ eV. A similar $c(4\times4)$ reconstruction with one or more heterodimers has been observed for pure GaAs surfaces, from STM studies and first-principles calculations.[18,34] Our results combined with these previous studies let us expect a similar heterodimer reconstruction to be observable on most of the III–V alloys. However, to our knowledge, no experimental observation of a $c(4\times4)$ reconstruction on In$_x$Ga$_{1-x}$As thin films has been reported in the literature so far. For In-rich alloy compositions, the film formation energy γ for the (2×3) reconstruction becomes comparable to that of the $\beta2(2\times4)$-In-seg. This leaves only a narrow range of conditions (very In-rich and As-rich) for its observation. The (4×3) reconstruction shows a higher γ than the (2×3) and $\beta2(2\times4)$-In-seg reconstructions for all relevant chemical potentials, indicating that it is absent under equilibrium conditions. The $\alpha(4\times3)$ and $\beta(4\times3)$ reconstructions observed for AlSb and GaSb surfaces[33] are also absent in the zero-temperature stability diagram (Fig. 3). Hence, they are unlikely to be observed for In$_x$Ga$_{1-x}$As films. Next we turn to the regions of the stability diagram corresponding to less As-rich conditions. For a moderate to high In chemical potential compared to that of Ga, the $\beta2(2\times4)$ and $\beta2(2\times4)$-In-seg reconstructions, respectively, become prevalent, while for high Ga chemical potential, the $\beta2(2\times4)$-Ga-seg reconstruction is the most stable one, as discussed above. Finally, at very low As chemical potential, we conclude from our calculations that the $\alpha2(2\times4)$ reconstruction with In segregation and with an In-As heterodimer on the surface (denoted as $\alpha2(2\times4)$-In-seg-InAs) is most stable for very In-rich alloy compositions, while the $\zeta(4\times2)$ reconstruction is most stable for Ga-rich alloy compositions.

For a film of known alloy composition, it is instructive to discuss the stability of reconstructions as function of μ_{As} alone, varying it, e.g., by annealing the film in the absence of further As supply. We consider three cases, the first one for

Ga and In incorporated in equal amounts, the second and third one for highly Ga-rich or highly In-rich alloy compositions, respectively.

In Fig. 5, we show the reconstructions likely to be observed for equal concentrations of the two cations ($\Delta\mu=0.4$ eV). We show the stability of various reconstructions as a function of As chemical potential, from a highly As-rich to an As-poor environment. The stable reconstructions with decreasing As chemical potential (higher annealing temperature) are (2×3), $\beta2(2\times4)$-In-seg, $\alpha2(2\times4)$-In-seg, and finally $\alpha2(2\times4)$-InAs.

Figure 6 shows the formation energy of reconstructions predicted for In-rich alloy films ($\Delta\mu=0.90$ eV). We find the $\beta2(2\times4)$ reconstruction with In segregation to be stable near the As-rich limit, however, with the (2×3) reconstruction being close in energy. For decreasing As chemical potential, this reconstruction is supplanted by the $\alpha2(2\times4)$-In-seg reconstruction, which is further followed by the $\alpha2(2\times4)$-InAs reconstruction. In the opposite extreme, for alloy films with Ga-rich composition ($\Delta\mu$
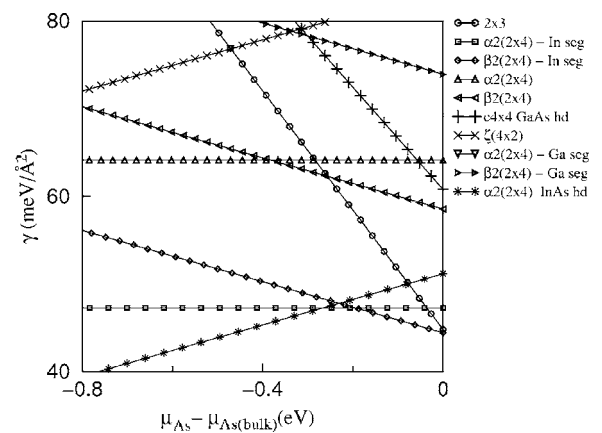

FIG. 6. Formation energies of some important and more stable reconstructions predicted for In-rich alloy films ($\Delta\mu=0.90$ eV). This corresponds to one vertical line from the stability diagram, Fig. 3 (the right y axis).

TABLE I. Formation energy γ [meV/Å^2] for $\mu_{In}-\mu_{In(bulk)}-(\mu_{Ga}-\mu_{Ga(bulk)})=0.4$ eV.

Reconstruction	$\mu_{As}-\mu_{As(bulk)}=0$	$\mu_{As}-\mu_{As(bulk)}=-0.6$
$\alpha2(2\times4)$-In-seg-GaAs	58.8	50.1
$\alpha2(2\times4)$-In-seg-InAs	56.6	47.9
$\alpha2(2\times4)$	56.8	56.8
$\alpha2(2\times4)$-Ga-seg	63.5	63.5
$\alpha2(2\times4)$-In-seg	50.9	50.9
$\alpha2(2\times4)$-Ga-seg-GaAs	68.7	60.0
$\alpha2(2\times4)$-Ga-seg-InAs	70.4	61.6
$\alpha2(2\times4)$-GaAs	63.5	54.8
$\alpha2(2\times4)$-InAs	61.6	52.9
$\beta2(2\times4)$-In-seg-GaAs-hd	56.9	56.9
$\beta2(2\times4)$-In-seg-GaGa-md	71.5	62.7
$\beta2(2\times4)$-In-seg-GaAs	65.6	56.8
$\beta2(2\times4)$-In-seg-InAs-hd	55.2	55.2
$\beta2(2\times4)$-In-seg-InIn-md	68.6	59.9
$\beta2(2\times4)$-In-seg-InAs	62.0	53.3
$\beta2(2\times4)$-In-seg-MDd	74.3	65.5
$\beta2(2\times4)$	51.3	60.0
$\beta2(2\times4)$-Ga-seg	55.7	64.4
$\beta2(2\times4)$-In-seg	48.1	56.8
$c(4\times4)$-GaAs-1hd	51.7	86.6
$c(4\times4)$-GaAs-3hd	83.0	100.5
$c(4\times4)$-InAs-1hd	51.3	86.2
$c(4\times4)$-InAs-3hd	78.6	96.1
$c(4\times4)$	51.5	95.2
2×4-GaAs	84.9	67.4
2×4-GaAs-In-seg	72.3	54.8
2×4-InAs	81.8	64.3
2×4-InAs-In-seg	70.2	52.7
$\zeta(4\times2)$	65.4	56.7
$\zeta(4\times2)$-In-seg	59.2	50.5
2×3	47.2	88.0
4×3	52.2	87.2
$\alpha(4\times3)$	58.6	76.1
$\beta(4\times3)$	52.9	87.9

TABLE II. Formation energy γ [meV/Å^2] for $\mu_{In}-\mu_{In(bulk)}-(\mu_{Ga}-\mu_{Ga(bulk)})=0.9$ eV.

Reconstruction	$\mu_{As}-\mu_{As(bulk)}=0$	$\mu_{As}-\mu_{As(bulk)}=-0.6$
$\alpha2(2\times4)$-In-seg-GaAs	57.0	48.3
$\alpha2(2\times4)$-In-seg-InAs	51.1	42.1
$\alpha2(2\times4)$	64.1	64.1
$\alpha2(2\times4)$-Ga-seg	81.7	81.7
$\alpha2(2\times4)$-In-seg	47.3	47.3
$\alpha2(2\times4)$-Ga-seg-GaAs	90.4	81.7
$\alpha2(2\times4)$-Ga-seg-InAs	85.1	76.4
$\alpha2(2\times4)$-GaAs	72.6	63.9
$\alpha2(2\times4)$-InAs	67.1	58.3
$\beta2(2\times4)$-In-seg-GaAs-hd	58.0	55.0
$\beta2(2\times4)$-In-seg-GaGa-md	71.5	62.7
$\beta2(2\times4)$-In-seg-GaAs	65.6	56.8
$\beta2(2\times4)$-In-seg-InAs-hd	49.7	49.7
$\beta2(2\times4)$-In-seg-InIn-md	61.4	52.6
$\beta2(2\times4)$-In-seg-InAs	54.7	46.0
$\beta2(2\times4)$-In-seg-MDd	70.6	61.9
$\beta2(2\times4)$	58.5	67.3
$\beta2(2\times4)$-Ga-seg	73.9	82.6
$\beta2(2\times4)$-In-seg	44.4	53.2
$c(4\times4)$-GaAs-1hd	60.8	95.8
$c(4\times4)$-GaAs-3hd	95.8	113.3
$c(4\times4)$-InAs-1hd	56.7	91.7
$c(4\times4)$-InAs-3hd	80.4	97.9
$c(4\times4)$	58.7	102.5
2×4-GaAs	94.0	76.5
2×4-GaAs-In-seg	66.9	49.4
2×4-InAs	87.3	69.8
2×4-InAs-In-seg	61.1	43.6
$\zeta(4\times2)$	83.7	74.9
$\zeta(4\times2)$-In-seg	55.6	46.8
2×3	44.8	85.6
4×3	49.8	84.8
$\alpha(4\times3)$	61.1	78.5
$\beta(4\times3)$	51.7	86.7

$=-0.10$ eV), Fig. 4 shows the formation energy as a function of μ_{As}. Our calculations show that the $\beta2(2\times4)$-Ga seg reconstruction is prevalent for high As chemical potential, while the $\zeta(4\times2)$ reconstruction prevails in the As-poor regime. We tested also cation-rich $\beta2(2\times4)$ reconstructions with cation-cation dimers (of same or different species). However, none of them is found to be energetically stable compared to the conventional reconstructions.

Tables I–III give numbers for the film formation energies of different reconstructions when In and Ga are present in equal concentrations, or for In-rich alloy films, or for Ga-rich alloy films, respectively. A few points are to be noted from these tables. It is observed that the pure $c(4\times4)$ reconstruction (As-As dimers only) and a variant with a single het-

erodimer (1HD) are very close in energy, however, the variant with a single heterodimer formed by Ga and As is the most favorable one. Among the $(n\times3)$ reconstructions, while all of them are close in energy, the (2×3) reconstruction is the most favorable and the $\alpha(4\times3)$ is the least stable one. It is also observed that the $\zeta(4\times2)$ reconstruction proposed by us is the most stable, with one In-In and two Ga-Ga subsurface dimers. From Table I, for high As chemical potential and $\Delta\mu \sim 0.4$, the (2×3) is seen to be the most stable reconstruction, closely followed by the $\beta2(2\times4)$-In-seg and the $\alpha2(2\times4)$-In-seg reconstructions, respectively. On the other hand, for low chemical potential of As, an $\alpha2(2\times4)$ reconstruction with In segregation and In-As heterodimer on top has lowest formation energy, followed by the $\alpha2(2\times4)$

TABLE III. Formation energy values γ [meV/Å^2] for $\mu_{In} - \mu_{In(bulk)} - (\mu_{Ga} - \mu_{Ga(bulk)}) = -0.1$ eV.

Reconstruction	$\mu_{As} - \mu_{As(bulk)} = 0$	$\mu_{As} - \mu_{As(bulk)} = -0.6$
$\alpha 2(2\times 4)$-In-seg-GaAs	60.7	51.9
$\alpha 2(2\times 4)$-In-seg-InAs	62.1	53.3
$\alpha 2(2\times 4)$	49.6	49.6
$\alpha 2(2\times 4)$-Ga-seg	45.3	45.3
$\alpha 2(2\times 4)$-In-seg	54.5	54.5
$\alpha 2(2\times 4)$-Ga-seg-GaAs	50.4	41.7
$\alpha 2(2\times 4)$-Ga-seg-InAs	52.4	43.7
$\alpha 2(2\times 4)$-GaAs	54.5	45.7
$\alpha 2(2\times 4)$-InAs	56.2	47.4
$\beta 2(2\times 4)$-In-seg-GaAs-hd	58.7	58.7
$\beta 2(2\times 4)$-In-seg-GaGa-md	71.5	62.7
$\beta 2(2\times 4)$-In-seg-GaAs	65.6	56.8
$\beta 2(2\times 4)$-In-seg-InAs-hd	60.6	60.6
$\beta 2(2\times 4)$-In-seg-InIn-md	75.9	67.2
$\beta 2(2\times 4)$-In-seg-InAs	69.3	60.5
$\beta 2(2\times 4)$-In-seg-MDd	77.9	69.1
$\beta 2(2\times 4)$	44.0	52.7
$\beta 2(2\times 4)$-Ga-seg	37.6	46.3
$\beta 2(2\times 4)$-In-seg	51.7	60.4
$c(4\times 4)$-GaAs-1hd	42.6	77.6
$c(4\times 4)$-GaAs-3hd	70.3	87.8
$c(4\times 4)$-InAs-1hd	45.8	80.8
$c(4\times 4)$-InAs-3hd	76.8	94.3
$c(4\times 4)$	44.2	87.9
2×4-GaAs	75.8	58.4
2×4-GaAs-In-seg	77.8	60.3
2×4-InAs	76.4	58.9
2×4-InAs-In-seg	79.3	61.8
$\zeta(4\times 2)$	47.3	38.6
$\zeta(4\times 2)$-In-seg	62.9	54.1
2×3	49.7	90.5
4×3	54.6	89.6
$\alpha(4\times 3)$	56.2	73.7
$\beta(4\times 3)$	54.1	89.1

reconstruction with In segregation and Ga-As heterodimer on top, and the $\zeta(4\times 2)$ reconstruction with In segregation, respectively. For In-rich alloy films and high As chemical potential (Table II), a $\beta 2(2\times 4)$ reconstruction with In segregation is the most stable one. This is closely followed by the (2×3) reconstruction and then the $\alpha 2(2\times 4)$ reconstruction with In segregation in the topmost cation layer. However, for low chemical potential of As, the $\alpha 2(2\times 4)$-In-seg-InAs reconstruction turns out to be most stable while the (2×4)-InAs-In-seg reconstruction is very close to it in surface energy. Hence under certain growth conditions, observing this reconstruction may be possible. This is in line with the observations of Schmidt et al.,[20] where this reconstruction has been reported for pure InAs. Table III gives values for the film formation energy for Ga-rich alloys $\Delta\mu \sim -0.1$.

For high As chemical potential, a Ga-segregated $\beta 2(2\times 4)$ reconstruction is most stable followed by the $c(4\times 4)$-GaAs-1hd and the $\beta 2(2\times 4)$ reconstructions, respectively. For low chemical potential of As, the $\zeta(4\times 2)$ reconstruction has the lowest formation energy, similar to pure GaAs(001). Hence, the possibility of observing the ζ reconstruction for In$_x$Ga$_{1-x}$As alloy films under In-poor condition awaits experimental verification.

B. Interplay of surface reconstruction and ordering

Next, we turn to investigations concerning the relation between the surface reconstruction and the type (CuPt$_A$ versus CuPt$_B$) of atomic ordering in the alloy films. We consider two indicators for the energetic preference associated with ordering: (i) the energy difference characteristic of the correlation between the surface reconstruction and the ordering type (surface-compatible ordering vs surface-incompatible ordering), (ii) the energetic preference for a particular cation species (In or Ga) occupying particular lattice sites of the topmost complete cation layer, either the one in accordance with the overall order in the film, or with In and Ga atoms interchanged.[1,2,38] For a surface terminated by As dimers, the smaller cation (Ga) prefers the subsurface site below the As dimers, while the more bulky In atom prefers subsurface sites in between As dimers (below a trench). If this pattern of site occupation is propagated from layer to layer during growth, it yields perfect ordering of either CuPt$_A$ or CuPt$_B$ type, depending on the surface reconstruction and its associated As dimer orientation. Hence, while criterion (i) selects the preferred ordering type, criterion (ii) provides a measure of the strength of the ordering to be expected. If the energy difference described by criterion (ii) is too small, a random alloy rather than an ordered structure would be formed at elevated temperatures due to entropic effects.

We have calculated the energy differences associated with (i) and (ii) for three exemplary cases, the $c(4\times 4)$-reconstructed surface with pure As dimers, the $\beta 2(2\times 4)$-In-seg reconstruction, and the $\zeta(4\times 2)$ reconstruction. To test criterion (i), we exchange the ordering pattern as a whole in all layers of the alloy film, keeping only the topmost reconstructed layers, involving a swap of all four In-Ga pairs in all three cations layers of our films, in total 24 atoms swapped. Tests of criterion (ii) involve a swap of all four In-Ga pairs in the first complete cation layer only, in total eight atoms swapped. While for the $\beta 2(2\times 4)$ and $\zeta(4\times 2)$ reconstruction the CuPt$_B$-type ordering is clearly favored (by 86 and 41 meV per cation, respectively), the $c(4\times 4)$ reconstruction shows a somewhat weaker preference for the CuPt$_A$ reconstruction (22 meV per cation). As mentioned already in the preceding section, these preferences are in line with the orientation of the As dimers and trenches in the respective reconstructions which determine the anisotropy of surface stress. For criterion (ii) describing the site-selectivity in the first complete cation layer of a given reconstruction, we find that the sites beneath the $c(4\times 4)$-reconstructed surface, in its ground-state CuPt$_A$ ordering, are highly selective with respect to occupation by In or Ga atoms (173 meV per cation). In the CuPt$_B$-ordered films with the $\beta 2(2\times 4)$ or the $\zeta(4$

$\times 2$) reconstruction, the selectivity for In versus Ga at the subsurface cation sites is lower, 36 and 140 meV per atom, respectively. These numbers should be compared with the free energy contribution stemming from configurational entropy in a random alloy. For an ideal alloy without any cation site preferences, this contribution is $k_B T \ln 2$. At temperatures of 500–600 °C typical for annealing experiments, the entropic contribution is therefore comparable to the site-selectivity energy. Hence, one would expect that realistic alloy films show only imperfect CuPt$_B$-type ordering, and indeed the experimentally observed degree of ordering is less than 100%.[2,39,40] It is also interesting to compare the selectivity energies of In$_x$Ga$_{1-x}$As with those of the more frequently investigated In$_x$Ga$_{1-x}$P alloy films on GaAs(001). According to previous studies,[38] the site selectivity in $\beta 2(2 \times 4)$-reconstructed In$_x$Ga$_{1-x}$As films with CuPt$_B$ ordering is about 20% lower than for the analogous In$_x$Ga$_{1-x}$P films (both lattice-matched with a suitable substrate). The reduction is in accordance with the trends in surface stress, with the shorter P-P dimers on In$_x$Ga$_{1-x}$P exerting more surface stress than the longer As-As dimers on In$_x$Ga$_{1-x}$As.

IV. CONCLUSION

In the present study, we have calculated the complete stability diagram of surface reconstructions on thin atomically ordered In$_x$Ga$_{1-x}$As alloy films on InP(001) substrate by means of density-functional theory calculations. In addition to the (2×3), $\beta 2(2 \times 4)$, and $\alpha 2(2 \times 4)$ reconstructions that have already been observed experimentally, our calculations show that a large part of the stability diagram, when the Ga concentration is higher than the In concentration, and the As chemical potential is low, is dominated by the $\zeta(4 \times 2)$ reconstruction known from pure GaAs(001) surfaces but hitherto unobserved for In$_x$Ga$_{1-x}$As alloys. For low chemical potential of As and high In concentrations, however, the $\zeta(4 \times 2)$ reconstruction is less stable than an $\alpha 2(2 \times 4)$ reconstruction with indium segregated to the subsurface layer. For even higher In concentrations, our calculations suggest that In-As heterodimers should occur on the surface of this reconstruction, in addition to the subsurface segregation of In. Moreover, we investigated the possibility of obtaining a $c(4 \times 4)$ reconstruction, either terminated purely by As dimers or with one or more heterodimers, for high values of the As chemical potential. While this reconstruction does not occur in the stability diagram, our calculations show that it is only slightly higher in energy, in particular the variant with one Ga-As heterodimer, than the prevailing (2×3) or $\beta 2(2 \times 4)$ reconstructions.

Concerning the cation ordering in the films, our calculations confirm the trends known from In$_x$Ga$_{1-x}$P films: The $c(4 \times 4)$ reconstruction, if stable, correlates with CuPt$_A$-type ordering in the films, while CuPt$_B$-type ordering is found to be energetically preferred for films with the $\beta 2(2 \times 4)$ and $\zeta(4 \times 2)$ reconstructions. Thus, CuPt$_B$-type ordering prevails even when the $\zeta(4 \times 2)$ appears. Quantitatively, the tendency to form ordered alloys in In$_x$Ga$_{1-x}$As alloy films is found to be somewhat weaker than in In$_x$Ga$_{1-x}$P alloy films.

[1] See MRS Bull. **22** (7) (1997).

[2] *Spontaneous Ordering in Semiconductor Alloys*, edited by A. Mascarenhas (Kluwer Academic/Plenum Publishers, New York, 2002), and references therein.

[3] A. Gomyo, K. Makita, I. Hino, and T. Suzuki, Phys. Rev. Lett. **72**, 673 (1994).

[4] L. Bellaiche, K. Kunc, M. Sauvage-Simkin, Y. Garreau, and R. Pinchaux, Phys. Rev. B **53**, 7417 (1996).

[5] M. Sauvage-Simkin, Y. Garreau, R. Pinchaux, M. B. Veron, J. P. Landesman, and J. Nagle, Phys. Rev. Lett. **75**, 3485 (1995).

[6] Y. Garreau, K. Aid, M. Sauvage-Simkin, R. Pinchaux, C. F. McConville, T. S. Jones, J. L. Sudijono, and E. S. Tok, Phys. Rev. B **58**, 16177 (1998).

[7] P. Kratzer, E. Penev, and M. Scheffler, Appl. Surf. Sci. **216**, 436 (2002).

[8] S. Ohkouchi and A. Gomyo, Appl. Surf. Sci. **130-132**, 447 (1998).

[9] B. A. Philips, I. Kamiya, K. Hinger, L. T. Florez, D. E. Aspnes, S. Mahajan, and J. P. Harbison, Phys. Rev. Lett. **74**, 3640 (1995).

[10] S.-H. Wei, L. G. Ferreira, and A. Zunger, Phys. Rev. B **41**, 8240 (1990).

[11] W. S. Han, B. Lee, J. H. Baek, J.-H. Lee, B. S. Jung, E.-H. Lee, and O. Byungsung, Appl. Phys. Lett. **72**, 1905 (1998).

[12] P. Ernst, C. Geng, F. Scholtz, H. Schweizer, Y. Zhang, and A. Mascarenhas, Appl. Phys. Lett. **67**, 2347 (1995).

[13] A. Gomyo, T. Suzuki, K. Kobayashi, S. Kawata, I. Hino, and T. Yuasa, Appl. Phys. Lett. **50**, 673 (1987).

[14] T. Suzuki, A. Gomyo, S. Iijima, K. Kobayashi, S. Kawata, I. Hino, and T. Yuasa, Jpn. J. Appl. Phys., Part 1 **27**, 2098 (1998).

[15] A. Zunger, S.-H. Wei, L. G. Ferreira, and J. E. Bernard, Phys. Rev. Lett. **65**, 353 (1990).

[16] S.-H. Wei and A. Zunger, Appl. Phys. Lett. **56**, 662 (1990).

[17] S. H. Lee, W. Moritz, and M. Scheffler, Phys. Rev. Lett. **85**, 3890 (2000).

[18] A. Ohtake, J. Nakamura, S. Tsukamato, N. Koguchi, and A. Natori, Phys. Rev. Lett. **89**, 206102 (2002); A. Ohtake and N. Koguchi, Appl. Phys. Lett. **83**, 5193 (2003); A. Ohtake, P. Kocan, J. Nakamura, A. Natori, and N. Koguchi, Phys. Rev. Lett. **92**, 236105 (2004); A. Ohtake, P. Kocan, K. Seino, W. G. Schmidt, and N. Koguchi, Phys. Rev. Lett. **93**, 266101 (2004).

[19] P. Vogt, K. Lüdge, M. Zorn, M. Pristovsek, W. Braun, W. Richter, and N. Esser, Phys. Rev. B **62**, 12601 (2000).

[20] W. G. Schmidt, F. Bechstedt, N. Esser, M. Pristovsek, Ch. Schultz, and W. Richter, Phys. Rev. B **57**, 14596 (1998); W. G. Schmidt, P. H. Hahn, F. Bechstedt, N. Esser, P. Vogt, A. Wange, and W. Richter, Phys. Rev. Lett. **90**, 126101 (2003).

[21] S. Froyen and A. Zunger, Phys. Rev. Lett. **66**, 2132 (1991); Phys. Rev. B **53**, 4570 (1996); S. B. Zhang, S. Froyen, and A. Zunger, Appl. Phys. Lett. **67**, 3141 (1995).

[22] P. C. Kelires and J. Tersoff, Phys. Rev. Lett. **63**, 1164 (1989).

[23] F. K. LeGoues, V. P. Kesan, S. S. Iver, J. Tersoff, and R. Tromp, Phys. Rev. Lett. **64**, 2038 (1990).

[24] A. Gomyo, M. Sumino, I. Hino, and T. Suzuki, Jpn. J. Appl. Phys., Part 2 **34**, L469 (1995).

[25] P. Hohenberg and W. Kohn, Phys. Rev. **136**, B864 (1964); W. Kohn and L. J. Sham, Phys. Rev. **140**, A1133 (1965).

[26] D. M. Ceperley and B. J. Alder, Phys. Rev. Lett. **45**, 566 (1980); J. P. Perdew and A. Zunger, Phys. Rev. B **23**, 5048 (1981).

[27] M. Bockstedte, A. Kley, J. Neugebauer, and M. Scheffler, Comput. Phys. Commun. **107**, 187 (1997).

[28] M. Fuchs and M. Scheffler, Comput. Phys. Commun. **116**, 1 (1999), and references therein.

[29] H. J. Monkhorst and J. D. Pack, Phys. Rev. B **13**, 5188 (1976).

[30] J. Neugebauer and M. Scheffler, Phys. Rev. B **46**, 16067 (1992).

[31] J. Tersoff, M. D. Johnson, and B. G. Orr, Phys. Rev. Lett. **78**, 282 (1997).

[32] The bulk phases with the lowest energy are used for the chemical elements, i.e., the orthorhombic crystal structure for Ga (α-Ga), the centered tetragonal structure for In, and the rhombohedral A7 structure for As.

[33] W. Barvosa-Carter, A. S. Bracker, J. C. Culbertson, B. Z. Nosho, B. V. Shanabrook, L. J. Whitman, H. Kim, N. A. Modine, and E. Kaxiras, Phys. Rev. Lett. **84**, 4649 (2000).

[34] E. Penev, P. Kratzer, and M. Scheffler, Phys. Rev. Lett. **93**, 146102 (2004).

[35] C. Kumpf, L. D. Marks, D. Ellis, D. Smilgies, E. Landemark, M. Nielsen, R. Feidenhans'l, J. Zegenhagen, O. Bunk, J. H. Zeysing, Y. Su, and R. L. Johnson, Phys. Rev. Lett. **86**, 3586 (2001).

[36] J. M. Millunchick, A. Riposan, B. J. Dall, C. Pearson, and B. G. Orr, Surf. Sci. **550**, 1 (2004).

[37] J.-H. Cho, S. B. Zhang, and A. Zunger, Phys. Rev. Lett. **84**, 3654 (2000).

[38] A. Chakrabarti and K. Kunc, Phys. Rev. B **68**, 045304 (2003); **70**, 085313 (2004); **72**, 045342 (2005).

[39] L. C. Su, I. H. Ho, and G. B. Stringfellow, J. Appl. Phys. **75**, 5135 (1994).

[40] D. Mao, P. C. Taylor, S. R. Kurtz, M. C. Wu, and W. A. Harrison, Phys. Rev. Lett. **76**, 4769 (1996).